Experimental Uptake Study of Ethanol by Water Droplets and Its Theoretical Modeling of Cluster Formation at the Interface

ARTICLE *in* THE JOURNAL OF PHYSICAL CHEMISTRY B · JUNE 2002

Impact Factor: 3.3 · DOI: 10.1021/jp015558n

3 AUTHORS, INCLUDING:

Stéphane Le Calvé
French National Centre for Scientific Research
90 PUBLICATIONS **996** CITATIONS

Experimental Uptake Study of Ethanol by Water Droplets and Its Theoretical Modeling of Cluster Formation at the Interface

Y. Katrib, Ph. Mirabel, and S. Le Calvé*

Centre de Géochimie de la Surface/UMR 7517 CNRS and Université Louis Pasteur, 1 rue Blessig, F-67084 Strasbourg, France

G. Weck and E. Kochanski

Laboratoire de Chimie Théorique/UMR 7551 CNRS and Université Louis Pasteur, 4 rue Blaise Pascal, BP 296, F-67008 Strasbourg, France

Received: October 10, 2001; In Final Form: March 7, 2002

Uptake measurements of ethanol were performed to provide experimental values for a theoretical approach of its incorporation into a water droplet. The uptake coefficients of ethanol on pure water were therefore measured as a function of temperature, using the droplet train technique coupled to a mass spectrometric detection. They were found to be independent of the aqueous phase composition and of the gas−liquid contact times. Their values show a negative temperature dependence, varying from 3.8×10^{-2} to 2.1×10^{-2} in the temperature range 266−280 K. From these kinetic data, the mass accommodation coefficient α was derived and was found to vary from 4.6×10^{-2} to 2.4×10^{-2} for the same temperature range. The results are used to discuss the uptake process involved in the incorporation of ethanol into an aqueous phase, using nucleation theory and quantum mechanical calculations. The small value of the experimental N* motivated calculations on very small clusters of the type ethanol−$(H_2O)_{n=1,3}$. This theoretical work shows the specific role of a cluster containing the ethanol molecule and only one water molecule. It could be a step toward either the growing of the cluster or its uptake by the surface of the droplet. Both the experimental and the theoretical works show that ethanol and methanol behave similarly.

Introduction

The uptake of organic or inorganic gaseous molecules by aqueous surfaces has been subject to many studies in the past decades.[1−6] Such studies are of great interest in atmospheric sciences where they are needed to predict the lifetime of soluble species. From a theoretical point of view, the uptake of a gas by a liquid is a challenging problem because it involves several steps. These steps mainly include diffusion in the gas and liquid phases, accommodation on the surface, saturation and reaction at the gas−liquid interface.

To describe the gas uptake process at the interface of a liquid, Davidovits et al.[1,7] developed a model based on the concepts of the classical heteromolecular nucleation theory. They suggested that the gas uptake proceeds via the formation of critical clusters which are formed in the dense gaslike interface region. If a molecule becomes part of such a critical sized cluster, then it will invariably be incorporated into the bulk. The critical cluster consists of a specific number of molecules *N**, which is the sum of the studied molecule plus the number of water molecules necessary to form a critical cluster. All substances do not have the same *N** value, and this number seems to depend on the structure of the molecule undergoing the uptake process and in particular, on the possibility to make hydrogen bonds with water. From experimental results, the *N** values are relatively small, ranging from approximately 1.5[8] to 6 for some carbonates[9] and these small values of *N** should allow quantum mechanical studies of cluster formation.

In the present work, we performed an experimental study, with the droplet train technique, of the uptake of ethanol by water surfaces as well as a theoretical modeling of cluster formation in the ethanol−water system. Uptake studies of ethanol have already been performed by Jayne et al.[10] and Shi et al.[11] However, Jayne et al.[10] pointed out some discrepancies in the results obtained for this alcohol, when compared with other alcohols such as MeOH, t-BuOH, 2-prOH, and 1-prOH. This is reflected in their Figure 8, where the curve for EtOH crosses the curves for the other alcohols. In addition, the *N** values for ethanol are in the order of 2.5[10] or 2.1 (this study) i.e., a critical cluster contains between 1 and two water molecules, allowing theoretical calculations. Indeed, additional information on the smallest clusters able to initialize the process can be obtained from quantum mechanical studies. The study of the most stable geometrical configurations, which play a dominant role in statistical analyses, allows the characterization of the nature and the magnitude of the interactions in the clusters. In particular, it can be related to *N** and to the corresponding energy.

Theoretical studies on the ethanol−water system are very scarce. Some recent works, based on molecular dynamics, are concerned with the liquid/vapor interface.[12−15] They examine, in particular, the orientation of the molecules at the surface of the liquid (bulk or droplet). These studies use simple analytical expressions to describe the inter and intramolecular potential, mentioning that "the results are naturally limited by the quality of the potential parameter used".[13] It is somewhat surprising that quantum mechanical calculations on ethanol−water het-

* To whom correspondence should be addressed.

10.1021/jp015558n CCC: $22.00
Published on Web 06/21/2002

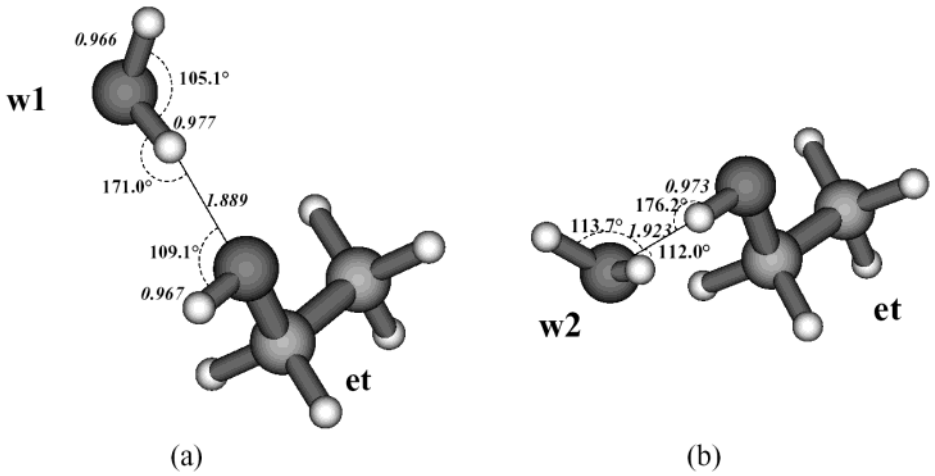

Figure 1. Optimized geometries of the ethanol-H_2O heterodimer at the DFT(B3LYP) level, using Basis S. Distances are in Å. The ethanol molecule can be proton acceptor (Figure 1a) or proton donor (Figure 1b).

erodimers appeared, to our knowledge, only in 1998.[16] This may be explained by the difficulties encountered in the quantum mechanical study of the methanol−water heterodimer, which should behave like the ethanol−water heterodimer. Due to the amphoteric nature of the hydroxyl groups, the alcohol and the water molecules can act both as hydrogen bond donors or acceptors. As a consequence, the alcohol molecule may be a proton acceptor (Figure 1a) or a proton donor (Figure 1b). In the case of the methanol−water heterodimer, early quantum mechanical calculations, performed at the Hartree−Fock level with a small basis set, favored the scheme of a proton donor methanol molecule,[17] whereas larger basis sets favor a proton acceptor methanol or nearly degenerate structure.[18,19] Simulations based on semiempirical parameters lead to similar uncertainties about the most stable structure.[20−22] In fact, the energy difference between the two structures was generally smaller than 1 kcal/mol. The question seems to get an answer from experimental work: in the gas phase, the proton donor methanol structure would be the most stable,[23,24] a similar result being obtained in argon matrix[25] but the reverse in nitrogen.[19] Accurate post-Hartree−Fock calculations are in agreement with these experimental conclusions.[16,26−29] However, getting the right answer from theoretical determinations is still a delicate task. Recent studies based on post-Hartree−Fock and DFT approaches,[16,26−29] eventually coupled with molecular dynamics studies,[30] show that not only the energy difference but even the relative stabilities of the two structures are method and basis set dependent. Two of these last studies also considered the methanol−water heterotrimers.[16,26] Fortunately, as will be shown in the present work, some uncertainties about the structure of the heterodimer do not affect that of the heterotrimer and have a rather minor energetic effect. This will be illustrated by our ab initio and DFT calculations performed on complexes involving the ethanol and one or two water molecules. To our knowledge, this work is the first quantum mechanical study on the ethanol−water heterotrimer.

To perform this study, we optimized the geometry of the most stable structures of the ethanol−H_2O heterodimer and ethanol−$(H_2O)_2$ heterotrimer. The calculation of the total intermolecular energy and its decomposition into terms of physical meaning have been done for both structures. This allows us to discuss the gas uptake process by a liquid in a more theoretical way, by trying to understand the cluster formation of ethanol and water molecules at the interface. We must underline that our theoretical work focuses on the formation of the cluster at the very early stage of the process. This step does not clearly appear in the molecular dynamics studies performed on this system.[12−15] Furthermore, some disagreements between the dynamic simulations studies and the experimental results show that the uptake of ethanol by water droplets is a very complex process involving several steps. We thus decided to first examine the very early steps of the formation of such a cluster.

Experimental Section

The uptake rate of a trace gas by a liquid is a multistep process that can be related to fundamental properties of the gas, interface or of the condensed phase such as the mass accommodation coefficient α, the solubility or the reactivity. The rate at which a trace gas molecule may be transferred into the condensed phase can be obtained from the kinetic theory of gases. The net flux Φ_{net} of a trace gas into a surface is expressed in terms of a measured uptake coefficient γ as

$$\Phi_{net} = \frac{1}{4}\langle c\rangle n\gamma \qquad (1)$$

where $\langle c\rangle$ is the trace gas average thermal speed, and n is the number density of the trace gas.

To measure uptake rates, we used the droplet train technique which has already been described elsewhere.[5,31] The uptake coefficient is determined by measuring the decrease of the gas phase concentration of the trace species, due to its exposure to a monodispersed train of droplets. These latter are generated by a vibrating orifice (70 μm diameter) leading to droplet diameters of about 140 μm. The apparatus, where the contact between both phases takes place, is a vertically aligned flowtube. The interaction time between the gas and the droplets can be changed from 0 to 20 ms either by moving the inner injector (up to 20 cm) or by changing the surface exposed by the droplet train (0−0.2 cm^2). In this last case, the change in surface of the droplet is achieved by changing the frequency applied to the vibrating orifice. Because the uptake process is directly related to the total surface S exposed by the droplets, any change ΔS in this surface results in a change of the trace gas density Δn at the exit ports of the flowtube. By considering the kinetic gas theory, the overall uptake coefficient γ_{meas} can then be obtained by measuring the fractional change of ethanol's concentration in the gas phase as a function of the total droplet surface, at a given temperature[32]

$$\gamma_{meas} = \frac{4F_g}{\langle c\rangle \Delta S}\ln\left(\frac{n}{n-\Delta n}\right) \qquad (2)$$

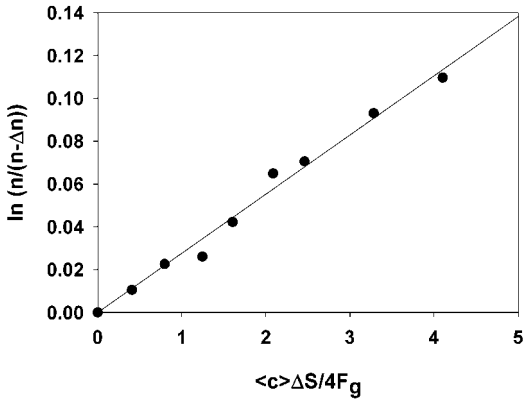

Figure 2. Typical plots of $\ln(n/n - \Delta n)$ versus $\langle c\rangle \Delta S/4F_g$ for ethanol on pure water at 275 K. According to eq 2, the slope is the uptake coefficient γ.

where F_g is the carrier gas volume flow rate, n and $(n - \Delta n)$ are respectively the trace gas density at the inlet and outlet port of the interaction chamber.

The uptake coefficient γ_{meas} can be measured as a function of the gas/liquid contact time, composition of the liquid used to produce the droplets or total pressure which was in the range 15−25 Torr. These last measurements are necessary to decouple the overall process into individual steps. An important aspect of this technique is the careful control of the partial pressure of water in the flowtube because it controls the surface temperature of the droplets through evaporative cooling.[32] Therefore, the carrier gas (helium) is always saturated, at a given temperature, with water vapor before entering the flow tube.

The gas stream coming out of the flowtube was analyzed using a differentially pumped mass quadrupole spectrometer Pfeiffer Vacuum QMS with an ionization energy of 60 eV. The signal was averaged over a second in order to increase the signal-to-noise ratio. Ethanol was monitored at 46 amu ($C_2H_5OH^+$) which corresponds to the molecular ion. In addition, H_2O and an inert tracer SF_6 were respectively monitored at 18 (H_2O^+) amu and 89 (S^+F_3) amu during the course of the experiments in order to see any potential perturbations in gas-phase concentrations.

Aqueous solutions used to prepare the droplets were made from Milli-Q water (18 MΩ cm). Ethanol (≥99.8%) was purchased from Carlo Erba and was used without further purification.

Experimental Results

A representative plot of $\ln(n/(n - \Delta n))$ as a function of $\langle c\rangle \Delta S/4F_g$ is shown in Figure 2, for the uptake of ethanol on pure water at 275 K. From eq 2, one can see that the slope of the curve gives the uptake coefficient γ_{meas} of ethanol at that temperature. The same procedure was used in the temperature range 266−280 K and the corresponding results are shown in Table 1. One can note from our results that the presence of NaOH has no influence on the observed uptake rates (see Table 1). Contrary to what has been observed by Jayne et al.[10] and Shi et al.,[11] we did not notice, under our experimental conditions, any saturation effect i.e., the uptake coefficients are independent of the gas−liquid contact time as shown in Figure 3.

The uptake rate of a trace gas by a liquid is known to be a function of several processes which include gas-phase diffusion, mass accommodation, solubility and reactivity in the liquid phase. Each of these processes may introduce a resistance (γ_{diff}, α, γ_{sat}, and γ_{rxn}) to the mass transfer from the gas phase into the aqueous phase and then the overall rate of uptake is obtained by summing up all these resistances.[33] In the absence of chemical reaction, the uptake coefficient may be described by[32]

TABLE 1: Measured Uptake, Calculated Diffusion and Saturation Coefficients, Mass Accommodation Coefficient of Ethanol as a Function of Temperature

T (K)	$10^2\gamma_{meas}$ ($\pm 2\sigma$)	$10^2\gamma_{diff}$	$10^2\gamma_{sat}$[b]	$10^2\alpha$ ($\pm 2\sigma + 5\%$)
265.8	3.82 ± 0.20	22.95	32.67	4.58 ± 0.28
267.5	3.60 ± 0.20	23.60	30.30	4.25 ± 0.26
267.7	3.10 ± 0.20	23.85	29.23	3.56 ± 0.26
268.9	3.29 ± 0.18	22.95	26.40	3.84 ± 0.24
269.9[a]	3.00 ± 0.09	22.00	25.65	3.47 ± 0.60
269.9	2.90 ± 0.10	22.00	25.63	3.34 ± 0.12
270.4	3.04 ± 0.14	22.85	24.15	3.51 ± 0.18
271.5	2.91± 0.28	22.95	22.62	3.33 ± 0.36
273.3[a]	2.60 ± 0.26	21.80	22.40	2.95 ± 0.33
273.8	2.46 ± 0.10	21.30	22.22	2.78 ± 0.12
274.7[a]	2.50 ± 0.10	20.25	18.24	2.85 ± 0.13
274.7	2.70 ± 0.10	20.25	18.20	3.12 ± 0.12
275.5	2.60 ± 0.08	21.00	17.54	2.97 ± 0.1
275.9	2.70 ± 0.12	20.41	15.87	3.11 ± 0.16
276.2[a]	2.65 ± 0.14	19.45	15.45	3.06 ± 0.20
276.2	2.40 ± 0.14	19.45	15.40	2.74 ± 0.20
278.0	2.30 ± 0.10	19.35	14.97	2.61 ± 0.12
279.0	2.50 ± 0.06	18.75	14.00	2.89 ± 0.08
280.5	2.10 ± 0.14	18.05	12.36	2.38 ± 0.20

[a] Experiments carried out using 0.1 M NaOH solution. [b] $1/\gamma_{sat}$ was calculated for a typical average contact time of 3 ms.

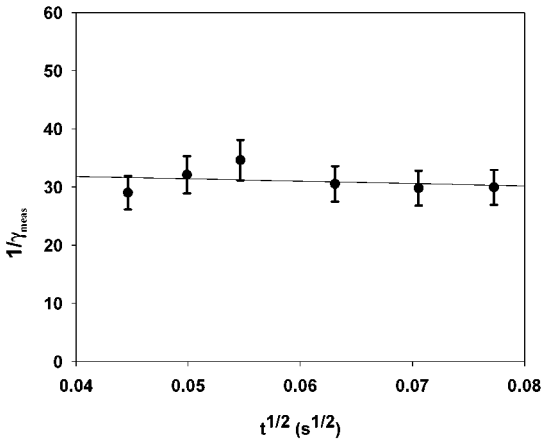

Figure 3. Typical plot of $1/\gamma_{meas}$ as a function of $t^{1/2}$ for ethanol on pure water at 269 K showing that γ was not a function of time within our experimental conditions. The error bars are given at the 2σ level.

$$\frac{1}{\gamma_{meas}} = \frac{1}{\gamma_{diff}} + \frac{1}{\alpha} + \frac{1}{\gamma_{sat}} \tag{3}$$

where

$$\frac{1}{\gamma_{sat}} = \frac{\langle c\rangle\sqrt{\pi t}}{8HRT\sqrt{D_a}} \tag{4}$$

and

$$\frac{1}{\gamma_{diff}} = \frac{\langle c\rangle d_{eff}}{8D_g} - \frac{1}{2} \tag{5}$$

In these expressions, H is the Henry's law constant, R is the perfect gas constant, T is the droplets temperature, D_a and D_g are the aqueous and gaz phase diffusion coefficients, d_{eff} the effective droplet diameter and t the gas/liquid contact time. In the above formula, only γ_{sat} shows a time dependence meaning

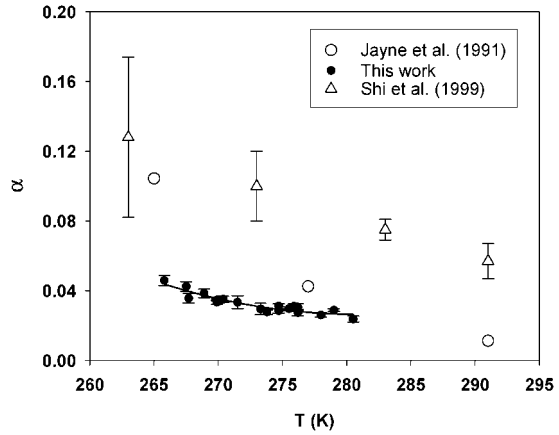

Figure 4. Plot of the mass accommodation α of ethanol versus temperature. Our results are reported along with the previous values obtained by Jayne et al. (1991)[10] and Shi et al. (1999).[11] The error bars are given at the 2σ level.

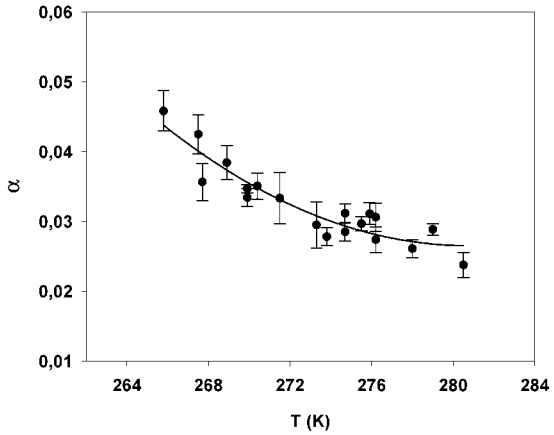

Figure 5. Plot of the mass accommodation α of ethanol versus temperature (This work). The error bars are given at the 2σ level.

that if $1/\gamma_{sat}$ is smaller than $1/\alpha + 1/\gamma_{diff}$, no time dependence should be observed experimentally.

Under our experimental conditions, the temperature T varies from 266 to 280 K, therefore the Henry's law constant H varies from 3100 to 800 M/atm[34] and the liquid-phase diffusion constant D_a from 5×10^{-6} to 9×10^{-6} cm^2 s^{-1}. For a typical average contact time of 3 ms, $1/\gamma_{sat}$ ranges from about 3 to 8 (see Table 1). This is of the same order of magnitude than $1/\gamma_{diff}$, but represents only 15% of the value of $1/\gamma_{meas}$, which is within the expected experimental uncertainties. The maximum value of $1/\gamma_{sat}$, obtained for $T = 280$ K and $t = 6$ ms, represents about 20% of $1/\gamma_{meas}$.

As mentioned above, Shi et al.[11] observed a time dependence for the global uptake of ethanol which decreases at lower temperatures. This decrease with T can easily be explained by the increasing solubility of ethanol at lower temperatures. For the highest temperature used, i.e., 291 K, H is about 334 M/atm,[32] leading to a value of $1/\gamma_{sat} = 27$ for $t = 9$ ms (their contact time goes up to 15 ms). This value now represents nearly 50% of their $1/\gamma_{meas}$ and therefore, it is not surprising that, in their case, a time dependence is observed for the highest temperatures. In Figure 4, we have plotted, for comparison, the three sets of experimental values for α (Jayne et al.,[10] Shi et al.[11] and the present work). Although our values are close to those of Jayne et al.[10] for the highest temperatures (well within experimental errors), large discrepancies appear for the lowest temperatures. Our α values, which are situated between those of methanol and 1-propanol seem to be more consistent, when considering the three alcohols. It should be noted that Jayne et al.[10] themselves found that the analysis of their ethanol data lead to some inconsistencies for the temperature dependence of the product $HD_1^{1/2}$.

Because our results show that the uptake coefficients are independent of the aqueous phase composition and of the vapor/liquid contact time, we can conclude that, under our experimental conditions the uptake rate of ethanol on water droplets is controlled solely by gas diffusion (γ_{diff}) and mass accommodation (α). Therefore, the uptake coefficient may be described according to[11]

$$\frac{1}{\gamma_{meas}} = \frac{1}{\gamma_{diff}} + \frac{1}{\alpha} = \frac{\langle c \rangle d_{eff}}{8D_g} - \frac{1}{2} + \frac{1}{\alpha} \qquad (6)$$

where the term $-1/2$ accounts for the distortion of the Boltzmann collision rate.[32] The gas-phase diffusion coefficient (D_g) needed have been estimated by the method of Reid et al.[35] The application of eq 6 was recently the subject of some discussion,[36,37] especially the diffusion correction formulation which is based on the work of Schwartz[38] who derived in a "simple but effective" manner the background leading to eq 6. As already underlined by several authors, most of the expressions describing the kinetics of mass transport are subject to some criticisms because of the assumptions made in their derivation. Therefore, the expression used to correct the measured uptake coefficients for gas phase diffusion limitations are only approximate. The Fuchs−Sutugin equation[39] is certainly the most widely employed equation for the description of mass transport in the Knudsen regime i.e., in the transition region from the continuum to the free-molecular regime. It is also valid for a wide range of experimental conditions. However, its derivation is less simple than the one made by Schwartz and therefore Schwartz's formulation is often preferred (such as in the present work). Using the expression for γ_{diff} derived by Hanson et al.[40] from the Fuchs−Sutugin treatment, one can easily show that under our experimental conditions, eq 6 is still valid. In our case (i.e., for pressures in the range 15−25 Torr) the deviation from the Fuchs−Sutugin formulation is less than 5% and for most experiments even less than 3%. This conclusion is similar to the one reached by Kolb et al.[36] We are confident that, under our experimental conditions, eq 6 can be adequately used in order to correct our raw data for potential mass transport limitations.

The employed estimation method has an average absolute error of about 5%[35] which will, under our experimental conditions, introduce an additional error of less than 5% in the mass accommodation coefficients.

Equation 6 may also be rewritten as follows

$$\frac{1}{\gamma_{meas}} - \frac{1}{\gamma_{diff}} = \frac{1}{\alpha} \qquad (7)$$

equation where the raw data ($1/\gamma_{meas}$) are corrected for gas-phase diffusion and which allows the direct determination of the mass accommodation coefficient α. In our conditions, the gas diffusion is less than 10% of $1/\gamma_{meas}$.

Table 1 summarizes the values of γ_{meas}, γ_{diff}, and α as a function of the temperature. The obtained mass accommodation values α decrease from 0.046 to 0.024 when the temperature increases from 266 to 280 K (Figure 5). This negative temperature dependence of α seems to be a general feature for the mass accommodation process of soluble nonreacting gases.[8] As noted previously, the uptake of ethanol by water surfaces

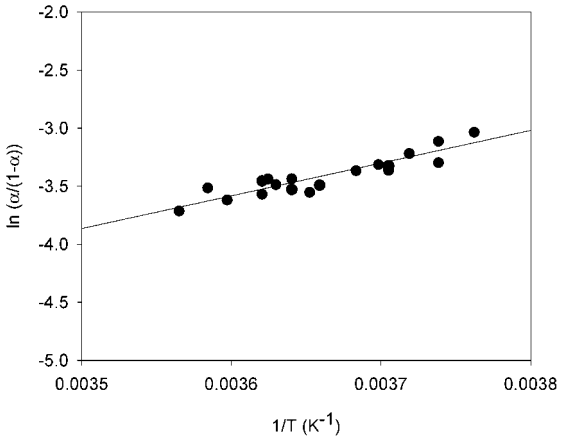

Figure 6. Plot of $\ln(\alpha/(1-\alpha))$ versus $1/T$. The slope of such a plot is $-\Delta H_{meas}/R$ and the intercept is $\Delta S_{meas}/R$.

has already been studied by Jayne et al.[10] Contrary to our results, a time dependent γ_{meas} was observed in their work, meaning that a saturation of the interface with ethanol was occurring. Taking into account this saturation effect, they obtained values for the mass accommodation coefficient α ranging from 0.104 to 0.011 between 265 and 291 K.

To explain the negative temperature dependence of α characterizing the interfacial transport, Davidovits et al.[1,7] developed a model suggesting that the gas uptake proceeds via the growth of critical clusters containing N^* molecules. They proposed the following equation

$$\frac{\alpha}{1-\alpha} = \exp\left(\frac{-\Delta G^*_{meas}}{RT}\right) \quad (8)$$

where the parameter ΔG^*_{meas} is the Gibbs free energy barrier between the vapor phase and the critical cluster. The values for ΔH_{meas} and ΔS_{meas} can be obtained by plotting $\ln(\alpha/(1-\alpha))$ versus $1/T$ (Figure 6). The slope of such a plot is $-\Delta H_{meas}/R$ and the intercept provides $\Delta S_{meas}/R$. The obtained values for ethanol are $\Delta H_{meas} = (-5.6 \pm 1.5)$ kcal mol^{-1} and $\Delta S_{meas} = (-27.4 \pm 5.5)$ cal mol^{-1} K^{-1}.

Using the classical nucleation theory, it is possible to link the thermodynamic parameters ΔH_{meas} and ΔS_{meas} to the critical cluster size N^*, representing the minimum value of N leading to efficient incorporation in the liquid[1,7]

$$\Delta H_{meas} = -10 \times (N^* - 1) + 7.53 \times (N^{*2/3} - 1) - 0.1 \times 10 \,(\text{kcal M}^{-1}) \quad (9)$$

$$\Delta S_{meas} = -13 \times (N^* - 1) - 19 \times (N^* - 1) + 9.21 \times (N^{*2/3} - 1) - 0.1 \times 13 \,(\text{cal M}^{-1}\,\text{K}^{-1}) \quad (10)$$

Using those two equations, we calculated a N^* value for ethanol equal to 2.1. The corresponding values of Jayne et al.[10] and Shi et al.[11] are $N^* = 2.5$ and 1.8, $\Delta H_{meas} = -11.0$ and -4.8 kcal mol^{-1}, $\Delta S_{meas} = -46.2$ and -21.9 cal mol^{-1} K^{-1}. Our results are in a better agreement with those obtained by Shi et al.[11] even if the mass accommodation coefficients are quite different. All of these results show that a critical cluster can be viewed as a cluster containing one ethanol molecule and either one or two water molecules.

Quantum Mechanical Calculations

Methods. Two categories of quantum mechanical methods are generally employed for the study of intermolecular interactions: the supermolecule treatment and the perturbation theory. They give complementary information and were both used in the present work.

In the supermolecule treatment, the full system is considered as one "supermolecule" and treated in the same way as one molecule at any level of the calculation: Hartree−Fock (HF), correlated, DFT, and so forth. The interaction energy is simply obtained by subtracting the energy of the monomers from that of the supermolecule. Of quite simple use, it gives a global number but does not allow to easily extract information on the nature of the interactions.

The perturbation method considers the intermolecular interaction energy as a perturbation correction to the total energy of the isolated subsystems. This interaction energy is decomposed into terms of physical meaning. The dominant contributions are the electrostatic, induction, dispersion, and their corresponding exchange terms. This method can give more information on the nature of the intermolecular interactions than the supermolecule treatment, but it requires specific sets of programs.

Computational Details. The Gaussian 98 package[41] was used for the treatment of the monomers and of the supermolecules. Ab initio calculations were performed at the Hartree−Fock and correlated levels. Several correlated methods were used, leading to close results. Only the CCSD(T) calculations (Coupled-Cluster Single and Double excitations with an appropriate inclusion of connected Triple excitations[42−45]) are reported in this paper. This approach is presently considered as the most accurate in this category to describe such hydrogen bonded systems.

For the DFT calculations, we selected the B3LYP functional, which gives rather good results for the study of the most stable structures of such systems.[46] The exchange functional B3 is a hybrid method proposed by Becke[47] that includes a mixture of Slater functional,[48] Becke's 1988 gradient correction[49] and Hartree−Fock-exchange. The correlation part LYP is the gradient corrected functional of Lee, Yang, and Parr.[50]

The program to compute the perturbation terms was written in our laboratory.[51] It provides the first-order electrostatic and exchange terms, and the second-order induction and dispersion contributions.[52] In the present stage of our work, the effect of the intramolecular correlation on the intermolecular interaction is neglected.

The geometries of ethanol [et], ethanol-H_2O [et−w1] and ethanol−$(H_2O)_2$ [et−w1−w2] were optimized at the DFT-(B3LYP) level using the basis set of Gaussian functions proposed by Sadlej.[53] This basis will be referred to as Basis S. It is a [10,6,4/5,3,2] GTO/CGTO basis for O and C and a [6,4/3,2] GTO/CGTO basis for H, especially built to correctly describe intermolecular interactions. For even better accuracy, this basis set was supplemented with three diffuse s functions and one diffuse p function on the oxygen atom. This more extended basis set, referred to as Basis S+, was used for the calculations of the energies. Furthermore, the basis set superposition error (BSSE) was corrected using the counterpoise correction:[54] the wave functions and energies of the monomers were computed with the basis set of the full system (heterodimer or heterotrimer).

Theoretical Results

(a) Geometries. The optimized geometries of the most stable structures of the ethanol−H_2O heterodimer and ethanol−$(H_2O)_2$ heterotrimer are shown in Figures 1 and 7. They are similar to those found for the methanol in interaction with water molecules.[16,26,30] We can also note that our optimized geometry of

TABLE 2: Total Interaction Energy for the Heterodimers and the Heterotrimer (kcal mol^{-1})

geometries:	heterodimer (Figure 1a)	heterodimer (Figure 1b)	heterotrimer (Figure 7)				
supermolecule:[a]	et−w1	et−w2	et−w1	et−w2	w1−w2	et−w1−w2	three-body contribution[b]
HF	−3.85	−3.29	−2.97	−2.48	−2.45	−10.63	−2.73
CCSD(T)	−5.38	−4.46	−4.54	−3.90	−3.58	−14.68	−2.66
DFT(B3LYP)	−5.03	−4.30	−4.48	−3.72	−3.70	−14.76	−2.86

[a] et = ethanol, w1 = first water molecule, w2 = second water molecule. The geometry of the heterodimers considered in the heterotrimer is taken from Figure 7. [b] The nonadditive three-body contribution is given by $E_{int}^{et-w1-w2} - E_{int}^{et-w1} - E_{int}^{et-w2} - E_{int}^{w1-w2}$.

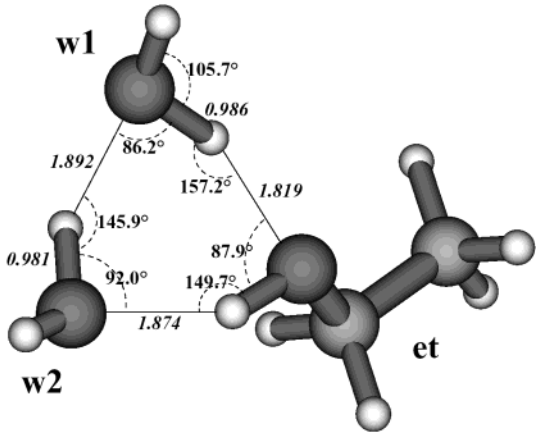

Figure 7. Optimized geometry of the ethanol−$(H_2O)_2$ heterotrimer at the DFT(B3LYP) level, using Basis S. Distances in Å.

the ethanol-$(H_2O)_2$ heterotrimer is rather close to that obtained for the water−trimer.[16] The ethanol molecule in the vacuum has a symmetry plan; in the most stable heterodimer and heterotrimer, the OH bond is out of the O−C−C plan by 1.2 and 4.1°, respectively.

The addition of a water molecule to the heterodimer leads to a three-molecule cycle (Figure 7) by the formation of a H-bond with the hydrogen atom of the alcohol group (similar to Figure 1b) and of a H-bond with the oxygen atom of the other water molecule. This induces a shift of the water molecule (w1) of the heterodimer toward the second water molecule (w2) and an increase of the OH bond length involved in the H-bond. This bond length is 0.967, 0.977, and 0.987 Å in the isolated molecule, in the heterodimer, and in the heterotrimer, respectively. The other OH bonds involved in H-bonds are also stretched. A stable four-molecule cycle structure of the ethanol−$(H_2O)_3$ cluster was also optimized.

As usual with DFT(B3LYP) calculations, the OH bond lengths are slightly larger than the experimental ones. However, this hardly affects the energies. The structure in Figure 7 shows that uncertainties about the most stable structures of the heterodimer cannot arise for the heterotrimer because both H-bonds (represented on Figure 1a and 1b) are present.

The geometry of the monomers is very slightly modified when they are involved in the heterodimer or the heterotrimer. The relaxation energy for the first water (w1), second water (w2) and ethanol (et) molecules in the heterotrimer is only 0.23, 0.26 and 0.18 kcal/mol, respectively. This gives a total relaxation energy of 0.67 kcal/mol, very close to the MP2 value (0.76 kcal/mol) reported for the methanol−water heterotrimer.[16]

(b) Total Intermolecular Energy: CCSD(T) and DFT-(B3LYP) Calculations. The intermolecular energy obtained from the supermolecule treatment is a small difference between numbers of the same order of magnitude. Reliable results require the calculations to be performed at the correlated level with a large basis set. The CCSD(T) method and the use of Basis S+ fulfill these conditions. Table 2 shows the overall agreement between the CCSD(T) and the DFT(B3LYP) results. The uncorrelated HF values, on the contrary, are systematically underestimated and show that the electronic correlation may contribute by as much as 36%.

The interaction energies found for the most stable structures of the ethanol−H_2O heterodimer are −5.4 kcal mol^{-1} (Figure 1a) and −4.5 kcal/mol (Figure 1b), respectively. These values are quite close to the counterpoise corrected values obtained at the MP2 level by Masella et al. (−5.3 kcal mol^{-1} and −4.4 kcal mol^{-1}, respectively, CP corrected)[16] and in the same range as those of similar accuracy published for the methanol−water heterodimer.[16,26] The interaction energy in the less stable heterodimer is also close to that of the water dimer (−4.5 kcal mol^{-1} in Masella et al.[16]). The energy difference between the two structures of the ethanol−water heterodimer is slightly larger than those reported in the literature for the methanol−water heterodimer with methods of similar accuracy.[16,26] This enhancement was also found by Masella et al.[16] and might be a characteristic of the alcohol. The heterodimers are slightly less bounded in the geometry of the heterotrimer (−4.5 and −3.9 kcal mol^{-1}). The interaction energy in the most stable heterotrimer (Figure 7) is −14.7 kcal mol^{-1}, again close to the CP corrected values reported by Masella et al.[16] (−14.3 kcal mol^{-1}) for the methanol−water heterotrimer. We can note that the corresponding value obtained for their water trimer is −13.9 kcal mol^{-1}. As seen above, these values are hardly affected by the geometrical relaxation of the monomers. These results show that the stabilization obtained by the addition of a second water molecule (about 9 kcal mol^{-1}) is much larger than that due to the addition of the first water molecule to the ethanol molecule.

We may note from the last column of Table 2 that the total intermolecular interaction energy in the heterotrimer is not strictly the sum of the intermolecular interaction energy between pairs of molecules. Nonadditive terms (cooperative effects) stabilize the total system by about 2.6−2.9 kcal mol^{-1}. This three-body contribution is already accounted for at the Hartree−Fock level. Again, this value is of the same order as in the methanol−water heterotrimer.[16,26]

Due to the close similarity between the methanol−water and ethanol−water systems, the potential energy surface of the ethanol−water heterotrimer is expected to be rather flat. Theoretical studies on transition states and saddle points of higher-order of the potential energy surface of the methanol−water heterotrimer[26] showed that the barriers associated with the flipping of the free groups (not involved in the H-bonds) are quite small, allowing easy tunneling processes. Such flat potential energy surfaces were also found for the methanol trimer[55] and the water trimer,[56] potential energy barriers due to the flipping of the free groups playing a negligible role in the attachment of the second molecule to the heterodimer.

We must underline that our quantum mechanical calculations are performed at 0K. An attempt to compute the zero-point energy (ZPE) gives a correction of about 2 kcal/mol at 298 K for the heterodimer. However, this correction is obtained with the use of a harmonic potential and the validity of this approximation to treat such intermolecular complexes may be questionable. Anharmonic potentials could be needed.[57] Furthermore, the value given above is obtained from a difference between large numbers of the similar order of magnitude. Though the ZPE correction is often included in calculations,[16,26] the accuracy of this determination is presently unknown and not considered here. We may note, however, that the zero-point and temperature corrections computed from vibrational frequencies estimated at the MP2 level[16] is only 0.3 kcal mol^{-1} for the ethanol−water heterodimer and 0.6 kcal mol^{-1} for the ethanol−water heterotrimer. Such small corrections would not affect the present analysis.

A four-molecule cycle is much more stable than the isolated heterotrimer and a third water molecule, the stabilization being even better than that of the heterotrimer with respect to the heterodimer and a water molecule. This is favored by both the pair interactions (the relative orientation of the four molecules to form H-bonds being more optimal than that of the three molecules in the heterotrimer) and the nonadditive contributions (more possibilities). This relative behavior will still be enhanced in larger clusters. The heterotrimer can be considered as an intermediate in the formation of an ethanol−$(H_2O)_3$ cluster, and more generally an ethanol−$(H_2O)_{n-1}$ cluster can be a step in the formation of a ethanol−$(H_2O)_n$ cluster. This does not exclude, of course, the possibility that an ethanol−$(H_2O)_{n-1}$ cluster can also grow by picking up more than one water molecule, for instance a water dimer.

In this analysis, the molecules are initially supposed in the gas phase region, not belonging to the interface, and far enough from it to have only weak interaction with it. Consequently, we do not consider the energy necessary to obtain free molecules from the interface: this entropically favorable step must take place before the formation of the critical cluster. As mentioned above, the potential hypersurface with respect to the flipping of the external groups (not involved in the H-bonds forming the three-members cycles) is flat for similar systems.[26,55,56] This deserves further comments: because the role of these groups is not important, the strong stability of the ethanol−water heterotrimer in gas phase should also occur if the second water molecule belongs to the interface, as long as both the oxygen and a hydrogen atoms are accessible. This condition, which implies that a free H atom of a water molecule of the interface points out of this interface, is commonly encountered.[58−60] For the same reason, two water molecules of the ethanol−$(H_2O)_3$ cluster could be two water molecules of the interface. This could be even more favorable because the strain would be smaller than in a three-members cycle. The mechanism involving the formation of a preliminary cluster composed of the ethanol and only one water molecule would be compatible with either the hypothesis of a growing cluster or with the accommodation of this small cluster by the surface of the droplet.

(c) Decomposition of the Interaction Energy in Terms of Physical Meaning: Perturbation Theory Calculations. As explained in the Methods section, the supermolecule treatment gives global numbers. It is relevant to also decompose these total interaction energies into terms of physical meaning, as done in the perturbation theory. This allows us to understand the nature of the interaction. The electrostatic energy is related to the electric multipoles of the monomers, the dispersion energy to the multipole polarizabilities, and the induction energy to both. Such a decomposition has never been proposed for these kind of alcohol−water systems.

TABLE 3: Dominant Contributions to the Interaction Energy (kcal mol^{-1})

geometries:	heterodimer (Figure 1a)	heterotrimer (Figure 7)			
A−B:[a]	et−w1	et−w1	et−w2	w1−w2	(et−w1)−w2
components					
electrostatic	−10.16	−11.58	−9.54	−9.28	−20.10
exchange	9.37	12.34	9.81	9.43	18.89
first order	*−0.79*	*0.77*	*0.27*	*0.15*	*−1.21*
induction (B → A)[b]	−2.23	−2.87	−1.87	−2.00	−3.54
induction (A → B)[b]	−1.16	−1.61	−1.55	−1.15	−3.62
total induction	*−3.39*	*−4.48*	*−3.42*	*−3.15*	*−7.16*
dispersion	−3.44	−3.75	−3.17	−2.79	−5.96
other terms[c]	2.23	2.93	2.41	2.22	

[a] et = ethanol, w1 = first water molecule, w2 = second water molecule. A is the first subsystem, i.e., et (columns 2−4), w1 (column 5) or the heterodimer et−w1 (last column). B is the second subsystem, i.e., w1 or w2. This means that the term (et−w1) of the last column corresponds to the heterodimer part of the heterotrimer, the energies of this column referring to the interaction between the two subsystems (et−w1) and w2. [b] B→A means that the subsystem B polarizes the subsystem A and creates an induced dipole moment on A (and the opposite for A→B). [c] Estimated from a comparison with the CCSD(T) values given in Table 2. They include many contributions (smaller than the dominant ones) such as the second-order exchange terms, the higher-order terms, the effect of the intramolecular correlation, etc.

The main components of this decomposition are given in Table 3. Results are presented for the most stable heterodimer (Figure 1a) and for the three pairs of molecules of the optimized heterotrimer. In the last column, we also consider the ethanol−first water molecule heterodimer (et−w1) interacting with the second water molecule (w2), in the geometry of the heterotrimer (Figure 7).

In all cases, the largest stabilizing term is the electrostatic contribution, which is similar for all the pairs (two H-bonds being involved in the case of the last column). This is probably due to the close dipole moments of the ethanol and water molecules (1.67 and 1.85 D at the MP2 level, respectively), with some variations involved by the relative orientations of the molecules. However, this large electrostatic contribution is mostly quenched by the first-order exchange term, such that the first-order contribution is quite small.

The comparison of the et−w1 pair in the heterodimer and in the heterotrimer shows that the increase of the electrostatic energy (−10.2 and −11.6 kcal/mol in the heterodimer and in the heterotrimer, respectively), is counterbalanced by an even larger increase of the exchange term (9.4 and 12.3 kcal/mol, respectively, due to the shortening of the H-bonds and the reorientation of the interacting molecules). This can lead to a repulsive first-order term. The total intermolecular energy (about −5 and −9 kcal/mol for the addition of the first and second water molecules, see previous section) is thus largely due to the other attractive terms (induction, dispersion). The polarizability of the molecule (4.9 and 1.4 Å^3 at the MP2 level for the ethanol and the water molecules, respectively), and not only the electric multipoles, plays a role in the stabilization of the full system. This is illustrated by the induction and dispersion energy values reported for the various pairs in Table 3.

A comparison of the two-body contributions in the heterotrimer deserves some comments. Table 2 shows that the et−w2 and w1−w2 contributions are close (in the worst case, they differ by 8%), and significantly smaller than the et−w1 one. This is not just due to artificial cancellations of errors since

this qualitative behavior is found for all the terms of the decomposition in Table 3, though with larger deviations in the case of the A→B induction (26%). This analysis shows that the et−w1 interaction remains favored in the heterotrimer, whereas the second water molecule w2 forms equivalent H-bonds with the ethanol and the first water molecule. This was also found for the methanol−water heterotrimer reported in Masella et al.[16] This can be understood from Table 1 and the values reported in Masella et al.[16] for the water dimer. Indeed, the interaction energy in a water dimer (4.47 kcal/mol if we include the BSSE correction[16]) is nearly equal to that of the heterodimer et−w2 (4.46 kcal/mol, Table 1), whereas that of the most stable heterodimer et−w1 is larger (−5.38 kcal/mol, Table 1). Such a favored interaction is not present in the water trimer (called cyc3 in Masella et al.[16]). Though the structure of all these trimers or heterotrimers is globally similar, that of the heterotrimer is less symmetrical than that of the water trimer. A favored interaction in the cycle is a characteristic of alcohols.

This section shows that several factors contribute to the stabilization of the systems. Though the global interaction depends on the molecular dipole moments and polarizabilities, it is difficult to deduce a direct correlation between the interaction energy and these molecular properties.

Discussion

It is interesting to notice that our experimental and theoretical work leads to complementary information, which are compatible, in particular for the following points:

− The N^* value (equal to 2.1) derived from our experimental results motivated our theoretical studies on small clusters involving an ethanol and one, two or three water molecules. The strong stability of the ethanol−$(H_2O)_{n=2,3}$ clusters and the minor role of the free groups suggest that a preliminary cluster composed of the ethanol and one water molecule could be a step toward either the growth of the cluster or the uptake of this cluster by the surface of the droplet. Indeed, the process may be more complex. However, we can note that the second mechanism would be compatible with both the experimental and the theoretical results.

− The specific role of an ethanol−water heterodimer appears in the geometric and energetic analysis. In its best geometry, the ethanol−water heterodimer is more stable than the water−water dimer. In the ethanol−$(H_2O)_2$ heterotrimer, one of the ethanol−water subsystem is more strongly H-bonded than both the other ethanol−water and the water−water subsystems. It was clearly shown by the total intermolecular energy and its decomposition into different energy contributions that the two water molecules do not display the same behavior in their interaction with the ethanol molecule: all the energetic components of the et−w2 subsystem are smaller than those of the et−w1 one, and generally comparable to those of the w1−w2 subsystem. A favored ethanol−water heterodimer can thus be identified in the heterotrimer, even if its geometric and energetic characteristics are slightly modified with respect to an isolated ethanol−water heterodimer.

−The experimental and theoretical results obtained in this work are similar to those previously obtained for the methanol−water system. Indeed, our experimental results can be compared to those obtained by Jayne et al.[10] for the experimental uptake study of methanol by water droplets. In addition, the optimized geometries and the total intermolecular energy, obtained for the ethanol−H_2O heterodimer and ethanol−$(H_2O)_2$ heterotrimer, are similar to those previously reported for the methanol−water system by Masella et al.[16] and Gonzalez et al.[26]

Conclusion

New experimental values for the uptake of ethanol by water droplet are presented together with theoretical studies on the ethanol−H_2O heterodimer and ethanol−$(H_2O)_2$ heterotrimer.

The nucleation theory we used in order to describe the gas uptake process at the gas−liquid interface suggests the formation of a critical cluster containing the ethanol molecule and only one water molecule, with an enthalpy formation of about 5−6 kcal mol^{-1}.

Quantum mechanical studies give complementary information on clusters of the type ethanol−$(H_2O)_{n=1,3}$ in gas phase. This work reports the first quantum mechanical calculations on the heterotrimer and heterotetramer. It also provides a decomposition of the interaction energy in terms of physical meaning for both the heterodimer and the heterotrimer. The theoretical work clearly shows that the interaction of one of the water molecules with the ethanol is favored. This suggests that a cluster involving the ethanol and only one water molecule may have a specific role. Globally, ethanol behaves like methanol in these systems.

Acknowledgment. Financial support for this experimental work has been provided by the French Ministry of Environment through the PRIMEQUAL program, the region of Alsace and the Centre National de la Recherche Scientifique (CNRS). The calculations were performed on our laboratory wokstations, at the Centre Universitaire Régional de Ressources Informatiques (CURRI) in Strasbourg, and at the Centre IDRIS (Project 01306) of the CNRS, Orsay, France).

References and Notes

(1) Davidovits, P.; Jayne, J. T.; Duan, S. X.; Worsnop, D. R.; Zahniser, M. S.; Kolb, C. E. *J. Phys. Chem.* **1991**, *95*, 6337−6340.
(2) Hanson, D. R.; Ravishankara, A. R. *J. Geophys. Res.* **1991**, *96*, 307−314.
(3) Jayne, J. T.; Davidovits, P.; Worsnop, D. R.; Zahniser, M. S.; Kolb, C. E. *J. Phys. Chem.* **1990**, *94*, 6041−6048.
(4) Kolb, C. E.; Worsnop, D. R.; Zahniser, M. S.; Davidovits, P.; Hanson, D. R.; Ravishankara, A. R.; Keyser, L. F.; Leu, M. T.; Williams, L. R.; Molina, M. J.; Tolbert, M. A. In *Advances in Physical Chemistry Series*; Barker, J. R., Ed.; World Scientific: Singapore, 1994; Vol. 3.
(5) Magi, L.; Schweitzer, F.; Pallares, C.; Cherif, S.; Mirabel, P.; George, C. *J. Phys. Chem. A* **1997**, *101*, 4943−4949.
(6) Schwartz, S. E.; Lee, Y. N. *Atmos. Environ.* **1995**, *29*, 2557−2559.
(7) Davidovits, P.; Hu, J. H.; Worsnop, D. R.; Zahniser, M. S.; Kolb, C. E. *Faraday Discussions* **1995**, 65−81.
(8) Nathanson, G. M.; Davidovits, P.; Worsnop, D. R.; Kolb, C. E. *J. Phys. Chem.* **1996**, *100*, 13 007−13 020.
(9) Katrib, Y.; Deiber, G.; Mirabel, P.; Le Calvé, S.; George, C.; Mellouki, A.; Le Bras, G. *J. Atmos. Chem.* **2001**, in press.
(10) Jayne, J. T.; Duan, S. X.; Davidovits, P.; Worsnop, D. R.; Zahniser, M. S.; Kolb, C. E. *J. Phys. Chem.* **1991**, *95*, 6329−6336.
(11) Shi, Q.; Li, Y. Q.; Davidovits, P.; Jayne, J. T.; Worsnop, D. R.; Mozurkewich, M.; Kolb, C. E. *J. Phys. Chem. B* **1999**, *103*, 2417−2430.
(12) Tarek, M.; Tobias, D. J.; Klein, M. L. *J. Chem. Soc., Faraday Trans.* **1996**, *92*, 559−563.
(13) Tarek, M.; Klein, M. L. *J. Phys. Chem. A* **1997**, *101*, 8639−8642.
(14) Taylor, R. S.; Ray, D.; Garrett, B. C. *J. Phys. Chem. B* **1997**, *101*, 5473−5476.
(15) Wilson, M. A.; Pohorille, A. *J. Phys. Chem. B* **1997**, *101*, 3130−3135.
(16) Masella, M.; Flament, J. P. *J. Chem. Phys.* **1998**, *108*, 7141−7151.
(17) Del Bene, J. E. *J. Chem. Phys.* **1971**, *55*, 4633−4636.
(18) Tse, Y.-C.; Newton, M. D. *Chem. Phys Lett.* **1980**, *75*, 350−356.
(19) Bakkas, N.; Bouteiller, Y.; Loutellier, A.; Perchard, J. P.; Racine, S. *J. Chem. Phys.* **1993**, *99*, 3335−3342.
(20) Bolis, G.; Clementi, E.; Wertz, D. H.; Scheraga, H. A.; Tosi, C. *J. Am. Chem. Soc.* **1983**, *105*, 355−360.
(21) Jorgensen, W. L. *J. Phys. Chem.* **1986**, *90*, 1276−1284.
(22) Kim, S.; Jhon, M. S.; Scheraga, H. A. *J. Phys. Chem.* **1988**, *92*, 7216−7223.
(23) Huisken, F.; Stemmler, M. *Chem. Phys. Lett.* **1991**, *180*, 332−338.
(24) Stockman, P. A.; Blake, G. A.; Lovas, F. J.; Suenram, R. D. *J. Chem. Phys.* **1997**, *107*, 3782−3790.

(25) Bakkas, N.; Bouteiller, Y.; Loutellier, A.; Perchard, J. P.; Racine, S. *Chem. Phys. Lett.* **1995**, *232*, 90−98.
(26) González, L.; Mó, O.; Yáñez, M. *J. Chem. Phys.* **1998**, *109*, 139−150.
(27) Tsuzuki, S.; Uchimaru, T.; Matsumura, K.; Mikami, M.; Tanabe, K. *J. Chem. Phys.* **1999**, *110*, 11 906−11 910.
(28) Jursic, B. S. *J. Mol. Struct. (THEOCHEM)* **1999**, *466*, 203−209.
(29) Kirschner, K. N.; Woods, R. J. *J. Phys. Chem. A* **2001**, *105*, 4150−4155.
(30) van Erp, T. S.; Meijer, E. J. *Chem. Phys. Lett.* **2001**, *333*, 290−296.
(31) Schweitzer, F.; Mirabel, P.; George, C. *J. Phys. Chem. A* **1998**, *102*, 3942−3952.
(32) Worsnop, D. R.; Zahniser, M. S.; Kolb, C. E.; Gardner, J. A.; Jayne, J. T.; Watson, L. R.; van Doren, J. M.; Davidovits, P. *J. Phys. Chem.* **1989**, *93*, 1159−1172.
(33) Jayne, J. T.; Duan, S. X.; Davidovits, P.; Worsnop, D. R.; Zahniser, M. S.; Kolb, C. E. *J. Phys. Chem.* **1992**, *96*, 5452−5460.
(34) Snider, J. R.; Dawson, G. A. *J. Geophys. Res.* **1985**, *90D*, 3797−3805.
(35) Reid, R. C.; Prausnitz, J. M.; Poling, B. E. *The Properties of Gases and Liquids*; McGraw-Hill: New York, 1987.
(36) Kolb, C. E.; Worsnop, D. R.; Jayne, J. T.; Davidovits, P. *J. Aerosol Sci.* **1998**, *29*, 893−897.
(37) Widmann, J. F.; Davis, E. J. *J. Aerosol Sci.* **1997**, *28*, 87.
(38) Schwartz, S. E. *NATO ASI Ser.*; Jaeschke, W., Ed.; Springer-Verlag: Berlin Heidelberg, 1986; 4, 415.
(39) Fuchs, N. A.; Sutugin, A. G. *International Reviews of Aerosol Physics and Chemistry*; Pergamon: New York, 1971; Vol. 2, 1−60.
(40) Hanson, D. R.; Ravishankara, A. R.; Lovejoy, E. R. *J. Geophys. Res.* **1996**, *101*, 9063−9069.
(41) Frisch, M. J.; Trucks, G. W.; Schlegel, H. B.; Scuseria, G. E.; Robb, M. A.; Cheeseman, J. R.; Zakrzewski, V. G.; Montgomery, J. A.; Stratmann, R. E.; Burant, J. C.; Dapprich, S.; Millam, J. M.; Daniels, A. D.; Kudin, K. N.; Strain, M. C.; Farkas, O.; Tomasi, J.; Barone, V.; Cossi, M.; Cammi, R.; Mennucci, B.; Pomelli, C.; Adamo, C.; Clifford, S.; Ochterski, J.; Petersson, G. A.; Ayala, P. Y.; Cui, Q.; Morokuma, K.; Malick, D. K.; Rabuck, A. D.; Raghavachari, K.; Foresman, J. B.; Cioslowski, J.; Ortiz, J. V.; Stefanov, B. B.; Liu, G.; Liashenko, A.; Piskorz, P.; Komaromi, I.; Gomperts, R.; Martin, R. L.; Fox, D. J.; Keith, T.; Al-Laham, M. A.; Peng, C. Y.; Nanayakkara, A.; Gonzalez, C.; Challacombe, M.; Gill, P. M. W.; Johnson, B. G.; Chen, W.; Wong, M. W.; Andres, J. L.; Head-Gordon, M.; Replogle, E. S.; Pople, J. A. *Gaussian 98*, revision A.5; Gaussian Inc.: Pittsburgh, PA, 1998.
(42) Purvis, G. D.; Bartlett, R. J. *J. Chem. Phys.* **1982**, *76*, 1910−1918.
(43) Scuseria, G. E.; Schaeffer, H. F., III *Chem. Phys. Lett.* **1988**, *152*, 382−386.
(44) Pople, J. A.; Head-Gordon, M.; Raghavachari, K. *J. Chem. Phys.* **1987**, *87*, 5968−5975.
(45) Raghavachari, K.; Trucks, G. W.; Pople, J. A.; Head-Gordon, M. *Chem. Phys. Lett.* **1989**, *157*, 479−483.
(46) Milet, A.; Korona, T.; Moszynski, R.; Kochanski, E. *J. Chem. Phys.* **1999**, *111*, 7727−7735.
(47) Becke, A. D. *J. Chem. Phys.* **1993**, *98*, 5648−5652.
(48) Slater, J. C. *Quantum Theory of Molecules and Solids*; MacGraw-Hill: New York, 1974; vol. 4.
(49) Becke, A. D. *J. Chem. Phys.* **1988**, *88*, 1053−1062.
(50) Lee, C.; Yang, W.; Parr, R. G. *Phys. Rev. B* **1988**, *37*, 785.
(51) Visentin, T.; Cézard, C.; Weck, G.; Kochanski, E.; Padel, L. *J. Mol. Struct. (THEOCHEM)* **2001**, *547*, 209−217.
(52) Kochanski, E. *Intermolecular Forces, The Jerusalem Symposium on Quantum Chemistry and Biochemistry*; Pullman, B., Ed.; Reidel: Dordrecht, 1981; Vol. 14, 15−31.
(53) Sadlej, A. J. *Collec. Czech. Chem. Commun.* **1988**, *53*, 1995−2016.
(54) Boys, S. F.; Bernardi, F. *Mol. Phys.* **1970**, *19*, 553−566.
(55) Mo, O.; Yanez, M.; Elguero, J. *J. Chem. Phys.* **1997**, *107*, 3592−3601.
(56) Fowler, J. E.; Schaefer, H. F., III *J. Am. Chem. Soc.* **1995**, *117*, 446−452.
(57) Valeev, E. F.; Schaefer, H. F., III *J. Chem. Phys.* **1998**, *108*, 7197−7201.
(58) Wilson, M. A.; Pohorille, A.; Pratt, L. R. *J. Chem. Phys.* **1988**, *88*, 3281.
(59) Matsumoto, M.; Kataoka, Y. *J. Chem. Phys.* **1988**, *88*, 3233.
(60) Townsend, R. M.; Rice, S. A. *J. Chem. Phys.* **1991**, *94*, 2207.